SAND77-1412
Unlimited Release

Solar Energy Research at Sandia Laboratories and Its Effects on Health and Safety

Lawrence L. Young, III

Prepared by Sandia Laboratories, Albuquerque, New Mexico 87115
and Livermore, California 94550 for the United States Department
of Energy under Contract AT(29-1)-789

Printed October 1977

Sandia Laboratories

SF 2900 Q(7-73)

DISCLAIMER

Issued by Sandia Laboratories, operated for the Department of Energy by Sandia Corporation.

Printed in the United States of America

Available from
National Technical Information Service
U. S. Department of Commerce
5285 Port Royal Road
Springfield, VA 22161

Price: Printed Copy $4.50; Microfiche $3.00

PAGES 1 to 2

WERE INTENTIONALLY

LEFT BLANK

SAND77-1412
Unlimited Release
Printed October 1977

SOLAR ENERGY RESEARCH AT SANDIA LABORATORIES AND ITS EFFECTS ON HEALTH AND SAFETY

Lawrence L. Young III
Safety Engineering Division 3442
Sandia Laboratories
Albuquerque, NM 87115

ABSTRACT

This paper discusses various solar energy research and development projects at Sandia Laboratories, with emphasis on the primary health and safety hazard associated with solar concentration systems. This limiting hazard is chorioretinal damage. We cannot yet measure the unique safety and health hazards associated with solar energy collector and receiver systems, but we are rapidly making progress. Research is continuing, especially for eye hazards, with more extensive work planned.

CONTENTS

ILLUSTRATIONS

SOLAR ENERGY RESEARCH AT SANDIA LABORATORIES AND ITS EFFECTS ON HEALTH AND SAFETY

Introduction

This nation has become increasingly concerned over the rapid depletion of conventional fossil energy resources. Achieving national energy independence has high priority, which in turn has stimulated a search for alternate energy sources and their development. Sandia Laboratories, a prime contractor to the U.S. Department of Energy (formerly known as the Energy Research and Development Administration), has led in developing and evaluating specific solar energy systems to economically harness this extensive source of electrical and thermal power.

Sandia Laboratories has established several solar facilities to develop, test, and evaluate the various solar components and subsystems that offer potential. These experimental projects will serve as unique prototypes and national engineering evaluation centers. Evaluation of various systems will provide empirical data to determine the areas of greatest potential for commercial applications.

In this report I present an overview of the major solar energy projects at Sandia Laboratories. The main emphasis is on the unique hazards associated with reflecting concentrated solar energy to a receiver. I do not discuss common industrial hazards associated with normal industrial settings, such as construction and high-pressure systems.

Solar Energy Research and Development Projects

Vertical-Axis Wind Turbine Power System

In addition to direct solar energy, Sandia Laboratories is also interested in harnessing solar-derived power from the wind.[1] The prime objective is to demonstrate the feasible advantages of a vertical-axis wind turbine power system in a power grid application. Two intermediate goals of such a system are

- An initial design and test device that will allow early total system investigations.
- A scale-up to a design comparable to the ERDA-funded 100-kW_e NASA-design horizontal-axis system, which will allow comparative judgments. The final goal is the design and installation of a megawatt-range system.

A prototype 17-m Darrieus Vertical-Axis Wind Turbine has already been constructed and is being tested in a two-blade configuration. Initial results have agreed with predicted structural and performance estimates.

Solar Total Energy Test Facility

The goals of the Solar Total Energy Test Facility[2] are

- Practical testing and evaluation of solar energy components and subsystems
- Development of an analytical and technological data base for further solar energy advances
- Evaluation of system interactions

- Identification of potential areas for research and development emphasis
- Simulation of operation modes for candidate solar total energy large-scale experiments
- Confirmation of analytical predictions of system performance
- Operational test bed for personnel training

Sandia's Solar Total Energy Test Facility is composed of two separate functions: the Solar Total Energy System Test Facility and the Solar Collector Module Test Facility.

Solar Total Energy System Test Facility -- The Solar Total Energy System Test Facility will use primary heat to generate 32 kW electrical power and up to 750,000 BTUs/hr of thermal energy for heating and air conditioning. The basic system will consist of solar collector fields, high- and low-temperature heat-storage tanks, fluid transfer systems, heat exchangers, an organic Rankine cycle turbine/generator, cooling tower, temperature and flow sensors, computerized controls and acquisition equipment, and support equipment that includes a complete weather station.

The Collector field consists of four different collector types, each of which provides approximately 24 percent of the solar power. Each collector field can function independently or with the other three fields.

1. The parabolic trough field designed by Sandia consists of four 60-ft-long parabolic troughs in two rows on an east-west axis. The collectors are front-surface reflectors made of aluminized Teflon laminated to Mylar and bonded to

aluminum sheets, then attached to the plywood trough. The stationary receiver tubes are coated with highly absorptive black chrome, sealed in evacuated black tubing and extended the full length of each set of troughs. A minicomputer sun-tracks and controls the collector field. Tracking is performed by comparing the collector elevation angle with a sun-position program for that specific day and then sending the correction signals to single-axis drive motors.

2. The parabolic dish is a three-collector array designed by Raytheon, Inc. The collector, a 22-ft segmented dish composed of silvered glass mirror surfaces, concentrates the solar radiation on a receiver mounted at the focal point. Nonabsorbing surfaces of the receiver are heavily insulated to prevent heat loss, and the receiver cavity is plated with black chrome on its absorptive surface. A computer controls tracking of the parabolic dish (like the parabolic trough), except that the dish has two-axis tracking.

3. The fixed mirror solar collector by General Atomic Company consists of precision-cast-concrete troughs with longitudinal silvered-glass facets. The two collector rows, each 200 ft long and 7 ft wide, are oriented on an east-west axis. Each row of collectors has a movable receiver assembly that tracks the sun's reflected and focused image. Changes in the sun's position are detected by special sun sensors that send signals to activate the receiver-tracking motor.

4. The Solar Linear Array Thermal System (SLATS), consists of two rows of reflectors, each 140 ft long x 10 ft wide. This system, designed by Sheldahl Company, is oriented on an east-west axis. Mirrored slats track the sun and concentrate the solar radiation onto a fixed receiver assembly. A sun sensor is also used in this system.

Two high-temperature storage systems maintain the temperature of the heat transfer fluid. The first storage system is a stratified single tank insulated by an evacuated jacket filled with multifoil insulation, 24 in. of bulk insulation at the top and bottom, and rock-wool bolts for the outer insulation of the tank. Capacity of the first storage system is 1300 gal. The second system consists of three 3000-gal tanks with bulk insulation.

The fluid transfer system interconnects all facility subsystems. The heat transfer fluid, Therminol-66 (T-66), circulates through the solar collector receivers, where it is heated to 400-600^{o}F. The heated T-66 is then pumped through insulated pipelines to the high-temperature storage tanks to be used later or directly to a toluene heat exchanger, where it becomes the energy source for boiling and superheating the toluene, which is the turbine/generator working fluid. After heating the toluene, the T-66 returns to the high-temperature storage tanks for recirculation through the collector fields.

The toluene heat exchanger is the interface between the heat transfer fluid (T-66) and the turbine working fluid (toluene). Heat exchange is accomplished in four phases: preheating, two boilings, and superheating. The toluene is heated to 588^{o}F and 275 psi and enters the turbine as superheated high-pressure gas. This superheated toluene expands through an axial-flow rotor to power the turbine/generator, which delivers a rated electrical output of 32 kW. When

the toluene is exhausted from the turbine/generator, it is cooled as it passes through a regenerator and a water-cooled condenser. The cooled toluene is pumped back to the heat exchanger for reheating.

The single-stage turbine/generator is driven at speeds up to 25,000 rpm by toluene gas. Reduction gears drive the generator at 1800 rpm to produce up to 32 kW of electrical energy. The turbine condenser coolant (water) is stored in a low-temperature storage tank and becomes the energy source for the heating and air-conditioning components of the system.

The Control and Equipment Center contains control and data acquisition equipment and is located in the same building as the toluene heat exchanger and the turbine/generator. The two low-temperature storage tanks, each with a 5000-gal capacity, store the heated condenser cooling water until needed for operation of heating or cooling components.

The induction-spray evaporative cooling tower dissipates excess heat from the turbine and absorption air-conditioner, and serves as part of the test load for systems under evaluation. The cooling tower can cool 350 gpm of water.

Solar Collector Module Test Facility -- The Solar Collector Module Test Facility test bed contains fluid test loops and instrumentation for testing individual concentrating collector modules. Either water or T-66 (heated to 630^{o}F and 2700 psi) can be used in the three test loops. The loops have pumping and cooling capacities adequate for collectors of about 500 ft^{2} maximum size.

Solar-Powered Irrigation System

Sandia Laboratories, along with ERDA and the State of New Mexico, has utilized one of the test collector designs to produce a solar-powered irrigation system.[3] This system will pump enough water to irrigate 100 acres of mixed crops, as well as supply a greenhouse and fish farm as part of an alternate season operation. The system, located on less than 4 acres of land, consists of a solar collector field of parabolic troughs, an energy storage tank, a solar engine, irrigation pump, controls, and a water storage pond.

This solar irrigation experiment was engineered and developed using available technology. Accumulation of data is important. Several temperature sensors and flow indicators have been incorporated into the system, and a small weather station monitors all environmental conditions. A multichannel data-recording unit will record data from the temperature sensors, flow indicators, and the weather station. The data will be used to analyze system performance. A 20-yr lifetime is the design goal for the system.

The solar engine, again an organic Rankine cycle/turbine, delivers 25-shaft horsepower to the irrigation pump. This pump will deliver 880 gpm from a well 75 ft deep during the 100-day irrigation season. A plastic-lined pond will store up to 4.5 acre-ft of water for demand as needed. Sun-tracking parabolic troughs heat the heat-transfer fluid to 420^{o}F. This preheated heat-transfer fluid is pumped into the collector field and heated in the parabolic trough receivers to 420^{o}F. There is 6,720 ft^{2} of reflective surface in the collector field. A control valve that is thermally controlled directs the hot fluid either to a thermal storage tank or to the boiler/heat exchanger.

In the heat exchanger, Freon R113 is heated to a gaseous state until it reaches a temperature of 325°F and a pressure of 220 psi. The heated high-pressure Freon gas drives the turbine that operates the irrigation pump. The Freon is then exhausted from the turbine and circulated through a regenerator heat exchanger and a condenser heat exchanger back through the cooling side of the regenerator heat exchanger and returned to the boiler/heat exchanger as a liquid.

The heat transfer fluid flows from the boiler/heat exchanger either back to the thermal storage tank or to a mixing tank. The mixing tank limits the temperature at which the fluid enters the solar collector receivers and helps control the temperature leaving the collector.

Water is taken from the storage pond for irrigation by a conventional pump that operates on demand to allow different types of irrigation equipment to be tested.

System operation is designed to be automatic, with a manual backup control system for emergencies. Collectors will be rotated to an upside-down position when the system is not operating. When the system is not operating the irrigation pump, it can generate 10,000,000 BTU/day of heat, or 200 kW/day electrical power.

Photovoltaics

Photovoltaics,[4] direct conversion of solar energy to electricity, is one of the newest technologies for trapping solar power and offers a promising method for major electrical power generation. Modern photovoltaic/thermal systems provide on-board power for many satellites.

Sandia Laboratories has a leading role in the national program of Systems Definitions Project. Long-term goals of the project are to identify promising applications for photovoltaic power generation systems as well as to establish optimum performance levels within practical economic limits.

Immediate objectives of Sandia's photovoltaic system are to

- Make conceptual design studies to identify photovoltaic systems worthy of further research and development
- Analyze systems and make related studies to gather information on performance, economics, legal factors, and environmental effects of large-scale power systems
- Establish design requirements and performance goals to guide development efforts toward low-cost systems and the use of new materials
- Provide system definition support to actual application and demonstration projects
- Define performance requirements for power generation systems and identify technical problem areas that require additional research to make systems perform to standards
- Initiate hardware experiments to establish the validity of analytical models, and confirm predicted performance

Sandia scientists are also experimenting with high-intensity solar cell development, called the photovoltaic/thermal system, which operates at high illumination and temperature levels and results in increased output efficiency. Cells under investigation include those made from silicon, gallium/arsenide, gallium/aluminum/arsenide, and other compound semiconductor materials.

Specific development of the high-intensity silicon solar cells has led to the design and construction of an advanced photovoltaic/thermal array enhanced with optical concentrators with the intent to trade expensive solar cell area for cheaper concentrator area. The array generates 1 kW_e and 5 kW_t power. A silicon solar cell 5 cm in diameter is the basis of the array. Each of the 135 cells in the array generates 7.4 W of power in full sunlight. Fourteen percent of the available sunlight falling on the photovoltaic/thermal array is directly converted to electricity, and an additional 50 percent is collected as heat, for a total radiation use of 64 percent. The array has a two axis-tracking system controlled by sun sensors.

A Fresnel lens system is the optical concentrator for the array. The lenses (which look like transparent, square phonograph records) are mounted in a framework at a fixed distance above the solar cells. They intensify the solar radiation on the cell surface 50 times, which in turn increases electrical output of each cell by a comparable amount.

Excess heat, which deteriorates solar cells, is removed by mounting the cells on collector tubing through which water is circulated. This prolongs cell life while providing hot water for space heating, air conditioning, and domestic or process hot-water supplies.

A cost comparison indicates that a nonconcentrating, 1-kW array of solar cells costs about $15,000 versus an estimated cost of $3,500 for the photovoltaic array enchanced with Fresnel lens concentrators. Analysts believe even more substantial cost reductions are possible. Current goals are to produce a system costing only $2,000/kW capacity by 1978 and to further reduce the system cost to $500/kW by the mid-1980s. These costs would make photovoltaic systems competitive with conventional power-generating methods.

Solar Thermal Test Facility (STTF)

Sandia Laboratories also boasts the largest Solar Thermal Test Facility in the world. The STTF is the major test facility for the national Solar Central Receiver Program.[5] While it is similar to the projected commercial solar thermal power plants, the STTF has a broad test capability for testing solar receivers (which have many similarities to conventional boilers) and heliostat fields. The STTF will also be used for materials evaluation, other energy conversion techniques, and unique chemical and metallurgical processes.

Major goals of the STTF are to provide experimental data for the design, construction, and operation of unique component systems for proposed solar thermal electric plants. The STTF project has a maximum thermal capacity of 5 MW_t and will emphasize scaled-down solar receivers and heliostats typical of those proposed for use in operational power plants.

Solar energy is collected and concentrated by sun-tracking heliostats. Each heliostat consists of 25 4- x 4-ft glass mirrors (facets) focused and aligned to produce a single concentrated beam of solar radiation at any desired test location on the central tower. Individual heliostats are also aligned with each other so that multiple heliostats produce a single three-dimensional spot at the focus and alignment point. The north sector heliostat field will contain more than 200 heliostats that will direct up to 5 MW_t of thermal solar energy on the tower receiver or other experiments. The site computer maintains positive beam control during heliostat operations.

Other prototype heliostat systems will also be evaluated at the STTF; all heliostat systems track the sun by using sun sensors and/or minicomputers for beam control. The central tower rises 200 ft and

contains three other test bays at 120-, 140-, and 160-ft levels in addition to the receiver location on the north face of the tower. The tower is served by a 100-ton capacity elevator and will also contain test instrumentation, heat rejection equipment, and a laser-scanning device used to focus the heliostats.

The thermal solar receiver may weigh up to 100 tons and extend up to 80 ft above the top of the tower. Each receiver will be different, with unique features that require specific testing. Water, steam, or air circulated through the receiver under test is heated to temperatures up to 1000^{o}F with resulting pressures up to 1400 psi. In an operational solar power plant, the high-temperature, high-pressure fluid would drive a conventional turbine/generator to produce electricity. A high-temperature storage incorporated into the system could assure uninterrupted power into the evening hours.

The STTF is expected to be completed by December 1977 at an estimated cost of $21 million.

HEALTH AND SAFETY HAZARDS ASSOCIATED WITH SOLAR CONCENTRATION SYSTEMS

Perhaps the most unique hazard associated with many solar collection systems is the reflection and reradiation of concentrated solar energy into the surrounding area. In most instances, this is a spectral reflection that occupies a distinct volume of space. The most sensitive parameter to this hazard is the retina of the eye. If the exposure of an unprotected eye is at a safe level, then all other parameters (e.g., skin, hair, and physical structures) are at a safe exposure level.

Anatomical and Physiological Properties of the Eye -- The retina is the most sensitive tissue of the mammalian body to solar radiation wavelengths of 400-1400 nm.[6] If all safety standards are defined in terms of retinal thresholds for unprotected eyes, then biological effects on all other tissues of the eye and skin will have been compensated for.

Let us briefly examine the gross anatomy and physiology of the eye as well as its associated optical parameters. Figure 1 shows a sagittal section of the eye with the major ocular components labeled. Light from a source such as the sun or an image of the sun reflected from a specular surface hits and transverses the ocular media. Light traveling through the ocular media is attenuated due to absorption, reflection, and scattering.[7] At the same time, light focuses into a smaller area. Therefore, power density on the retina may be different from density at the cornea.

The first anatomical structure the light hits is the cornea, which is not transparent to far ultraviolet radiation (UV) but is

EYE (SAGITTAL SECTION)

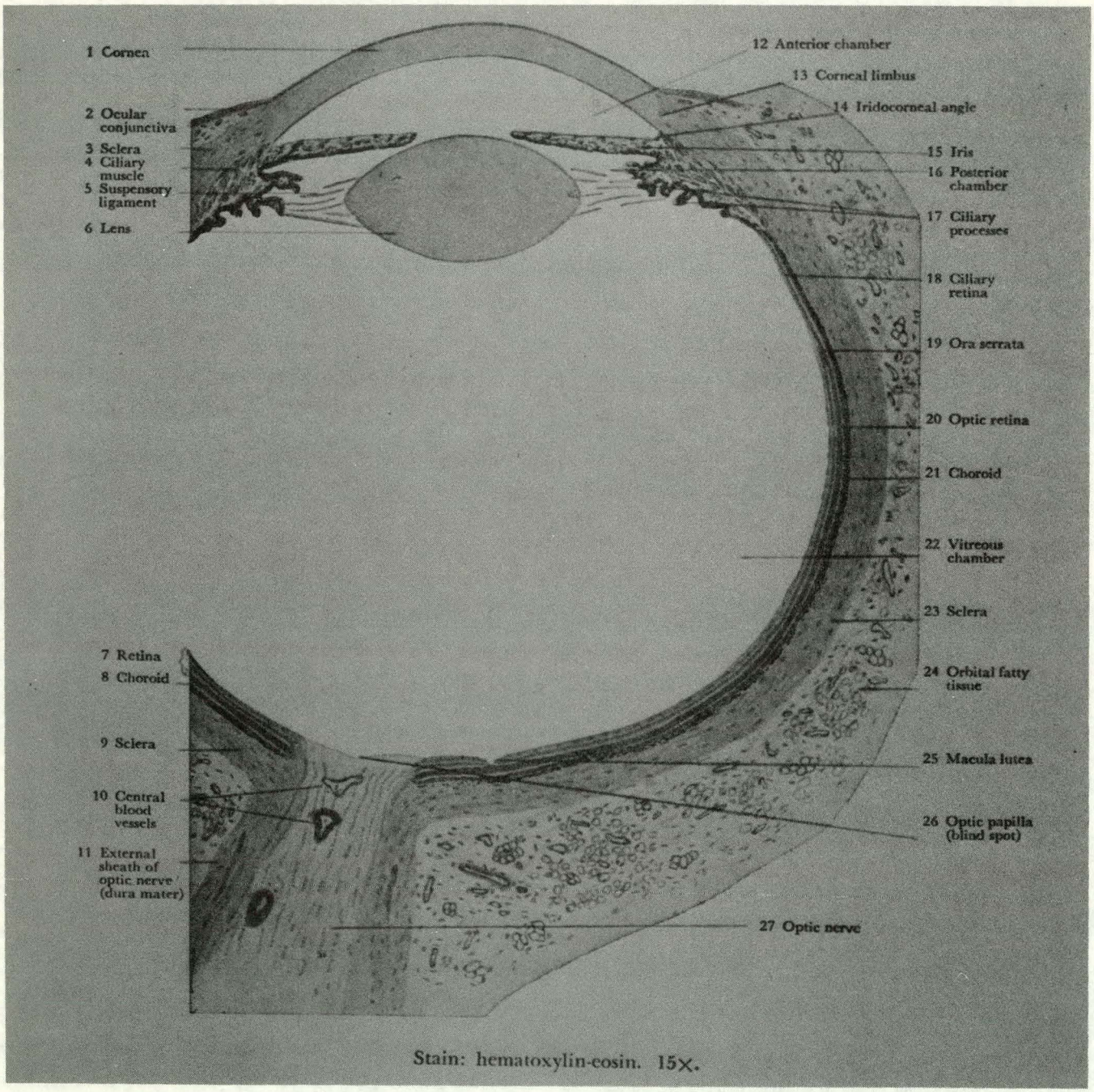

Fig. 1 Extracted from Di Fiore, M.S.H. Atlas of Human Histology 4th ed., Lea & Febiger, Philadelphia, 1974

transparent to light of longer wavelengths into the infrared. The cornea is the main refractive element of the eye. The next structure encountered is the acqueous humor, which is transparent to light in the UV, visible, and near-infrared spectra. The amount of light entering the rest of the eye is limited by the iris and its asso-ociated pupillary opening, which controls the total amount of light reaching the retina.

The lens, the next structure to be traversed, is responsible for the finite focusing ability of the eye (accommodation). The lens is transparent to wavelengths from 400-1400 nm.

The largest component of the eye is the vitreous humor, a gel-like material behind the lens that is transparent to most of the light from 350-1300 nm.[7] After passing through the ocular media, the light finally reaches the retina. About 74-77 percent of the light that is incident on the cornea and has an adequate angle to pass through the pupillary opening actually reaches the retina.[8]

The retina is virtually transparent to light. An estimated 10 percent or less of the light incident on the retina is absorbed by visual pigments and neural structures of the retina. The rest of the light is absorbed by the pigmented layer separating the retina from the choroid.[7]

When light enters the retina, it must pass through two layers of neural cells before it strikes the photoreceptor cells (Figure 2). These photoreceptor cells, known as the rods and cones, contain the visual pigments and transduce photo stimuli into electrical impulses that travel to the brain by the optic nerve tract. Directly below the rods and cones lies the pigmented epithelium of the retina. The retinal pigmented epithelium prevents backscatter of the photons by absorbing them.

RETINA & CHOROID OF THE EYE

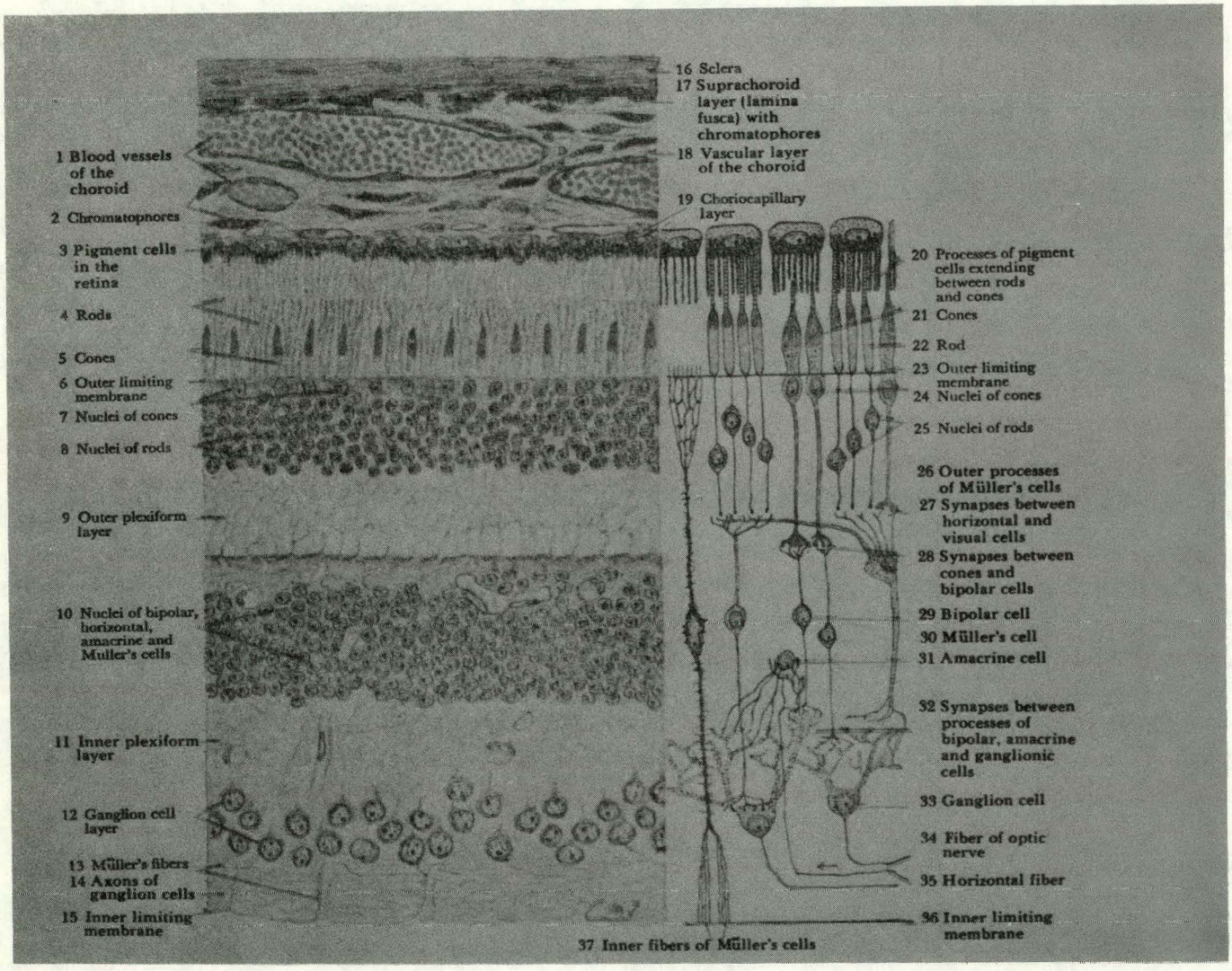

Fig. 2 Extracted from Di Fiore, M.S.H. Atlas of Human Histology, 4th ed., Lea & Febiger, Philadelphia, 1974

The retina and its associated pigmented epithelium contain few blood vessels and therefore have a decreased ability to dissipate heat. The major blood supply and resulting heat-dissipating mechanism are contained in the choroid, which lies immediately under the retinal pigmented epithelium.

Optics -- Optical properties of the eye play an important role in determining chorioretinal injury parameters. Factors to consider are retinal image size, pupil size, spectral absorption, and scattering by the ocular media; irradiancy of the source; and reflectivity of the reflective surface. Perhaps the best way to approach the subject is to discuss the relationship between external focusing systems and the optical focusing system of the eye, thus relating skin or corneal radiation intensities with retinal irradiation.

In focusing phenomena, the closer an external target is to the reflective surface in front of the focal point (or the farther away beyond the focal point) the larger the image is on the target (Diagram A). But this is not true on the retina of the eye. Retinal image size is largest at the focal point, becoming smaller with an increase in distance from the focal point (Diagram B). When the eye is at the focal point, the complete reflective surface is filled with the sun's image. As the eye moves away from the focal point, the beam size becomes larger, and the pupillary opening can see only part of this beam at any one time (Diagram C). Therefore, the apparent image size of the sun on the reflective surface, as perceived by the eye, becomes smaller.

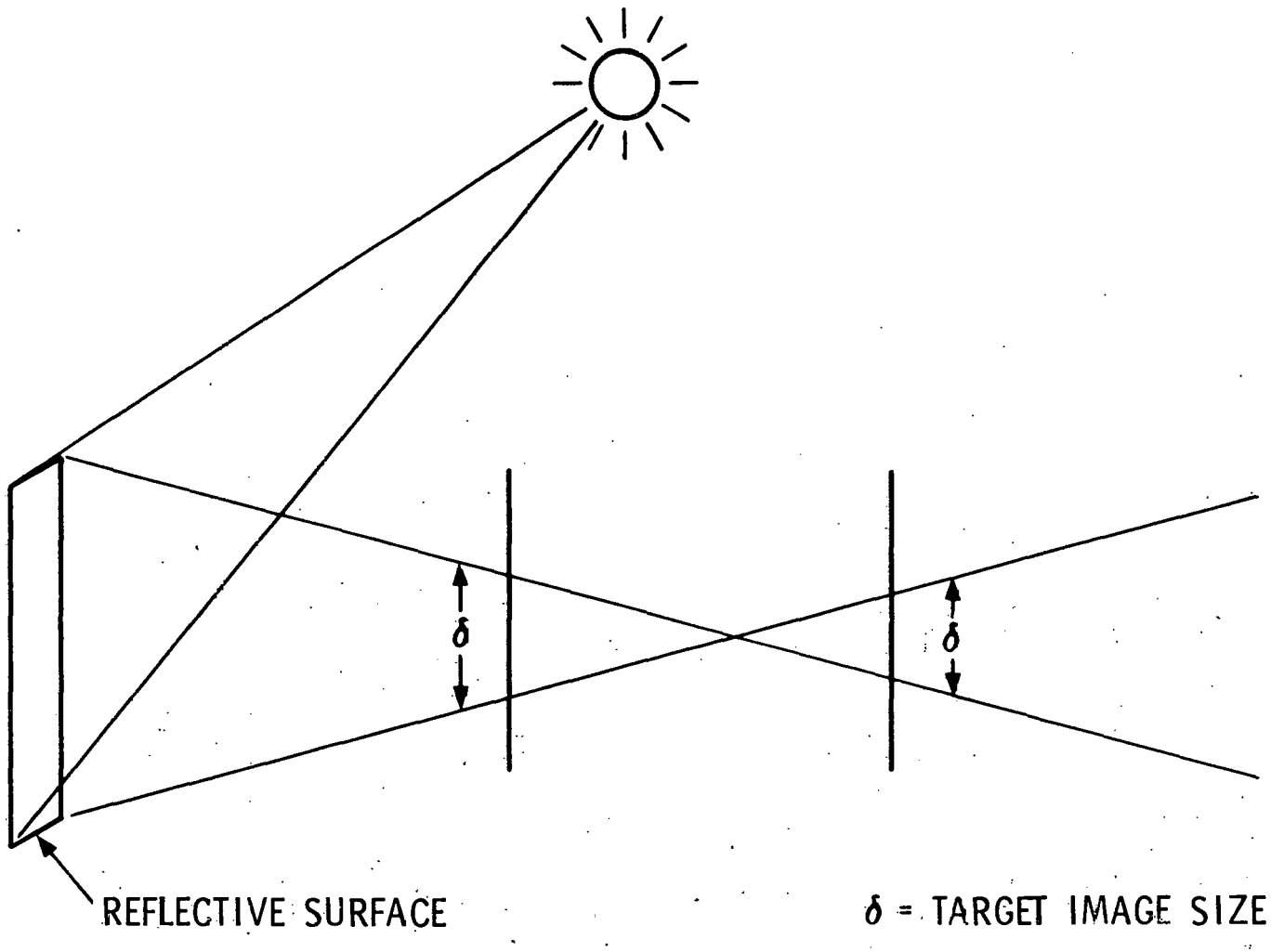

Diagram A. Differences in image size on external target in a focusing system

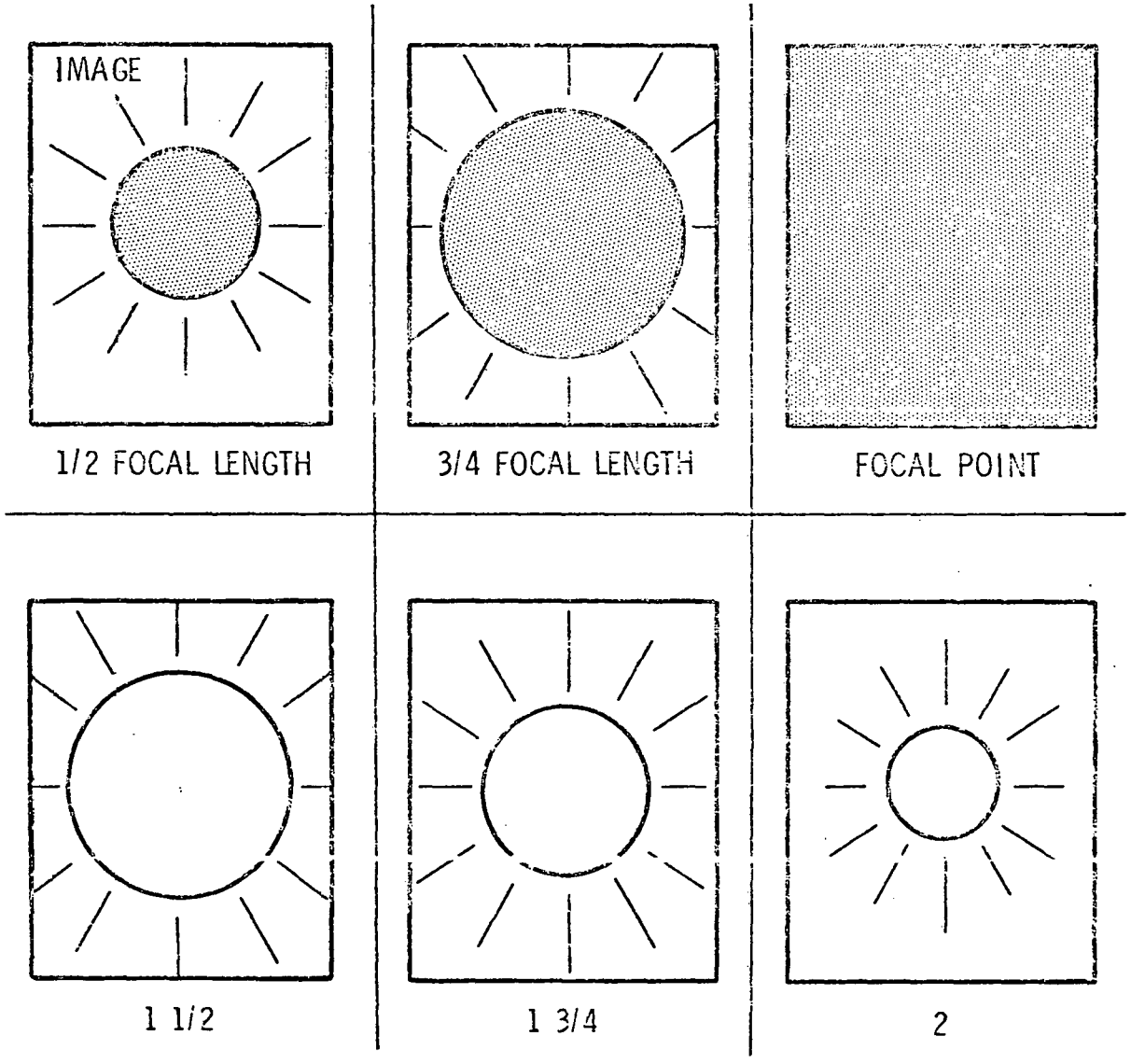

Diagram B. Differences in retinal image size with eye in a focusing system

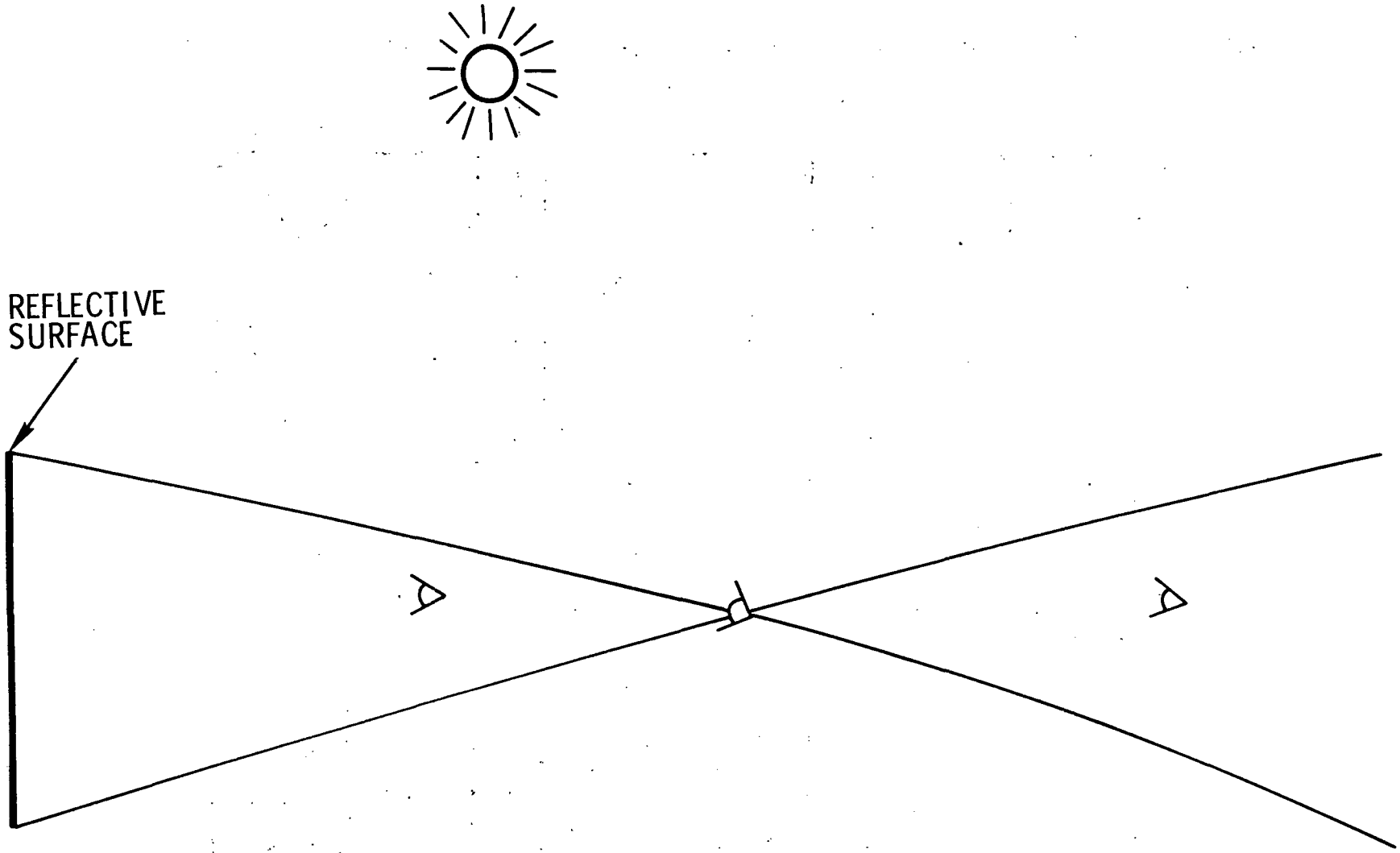

Diagram C. Different locations of eye in image beam from fccusing system

For a nonfocusing external system, on-axis as one moves away from the source, radiation intensity at the cornea decreases as the square of the distance. Simultaneously, the intensity of energy on the retina remains constant (ignoring scattering and attenuating due to relatively short distances), and the retinal image size becomes smaller.[9]

From this, we can extrapolate that, in an on-axis focusing system, as the eye moves closer to the focal point corneal irradiance increases, the retina image size increases, and the retinal irradiance remains constant. On the other hand as the eye moves away from the focal point, corneal irradiance and retinal image size become smaller, and the retinal irradiance continues to remain constant. Therefore, (given a constant source and ignoring atmospheric attenuation) retinal image size and the intensity of energy on the cornea may change, but the intensity per unit area on the retina remains the same. This change in retinal image size and corneal irradiance is known to be true.[10] The theory that the on-axis retinal intensity per unit area remains constant is commonly accepted but has not yet been proved.

Frank Biggs, Gene Igles, Clarence Robertson, and L. L. Young, all of Sandia Laboratories, are experimenting to determine whether retinal irradiance per unit area is indeed a constant. Indications are confirming this commonly held theory. Ignoring atmospheric attenuation is a valid procedure considering the short distances we are considering.

Threshold Values -- By the law of conservation of brightness, no optical system can increase the brightness of a light source. Thus retinal irradiance cannot be brighter than irradiance resulting from direct viewing of the source (in this case, the reflected image of the sun as opposed to direct viewing of the sun). If we know the damage threshold to the retina and all the variable parameters associated, we can arrive at safe exposure levels tolerable by humans. Let us now look at these variable parameters.

The pupil, which is the limiting aperture of the eye, determines the total amount of radiant energy entering the eye. Energy entering through the pupil, and therefore reaching the retina, is proportional to the area of pupillary opening. For the normal outdoor daylight adapted eye, the normal pupil diameter will be 2-3 mm, and momentary viewing of the sun causes the pupil to constrict to approximately 1.6 mm.[11]

Most light energy reaching the retina is absorbed by the pigmented epithelium and converted to heat. Due to the poor heat-removal mechanism of the retina, given a constant irradiancy from a source, the image size on the retina is the most important parameter in initiating thermal damage (chorioretinal burn) for exposures of short duration.

The angle subtended by a single extended source defines the retinal image size. The retinal image size (d_r) can be calculated if ones knows the effective focal length of the relaxed eye (f $\sim$1.713 cm), the viewing distance (r, in cm), and the dimension of the light source, $\left[D_L, \text{ in meters } D_L = \frac{4(\text{Area})}{\text{perimeter}}\right]$.

$$d_r = \frac{D_L f}{r} \qquad \text{(Reference 10)} \qquad (1)$$

This formula does not hold for very large angles (5 % error at 60°).

Radiance of the solar reflecting source (L, in $w/cm^2 \cdot sr$), can be calculated if solar insolation (q, in w/cm^2) reflectivity of the solar reflector (n), and the half-divergence angle (β, $\sim 4.66 \times 10^{-3}$ rad) are known.

$$L = \frac{qn}{\pi\beta^2} \tag{2}$$

This value is important in computing the theoretical retinal irradiance, E_r. Theoretical retinal irradiance is a function of pupillary diameter in cm *(d_p), radiance of the source (L), transmissivity of the ocular media (τ, ~ 0.74), the percentage of solar insolation between 400-1400 nm (ν, ~ 0.88), and the ocular focal length in cm (f).[10] E_r is expressed in $watts/cm^2$.

$$E_r = (\pi \cdot d_p^2 \cdot L \cdot \tau \cdot \nu)/4f^2 = 0.27 d_p^2 \cdot L \cdot \tau \cdot \nu \tag{3}$$

For most computations this equation can be used for a single-source image. Once the equipment has been built, one could measure corneal irradiance and compute retinal exposure for a particular solar insolation by the following equation:[10]

$$E_r = \frac{\tau \cdot E_c \cdot \nu\left[\left(\pi d_p^2\right)/4\right]}{A_r} \tag{4}$$

where

τ = ocular transmissivity (~ 0.74)
E_c = corneal irradiance
ν = percent of radiation between 400-1400 nm (~ 0.88)
*d_p = pupillary dimeter in m
A_r = retinal image area
E_r = retinal irradiance, in $watts/cm^2$

*Note: In equation (3) d_p must be given in centimeters (cm) while in equation (4) d_p must be given in metres (m).

THIS PAGE

WAS INTENTIONALLY

LEFT BLANK

TYPICAL LIGHT SOURCES AND EYE DAMAGE THRESHOLDS

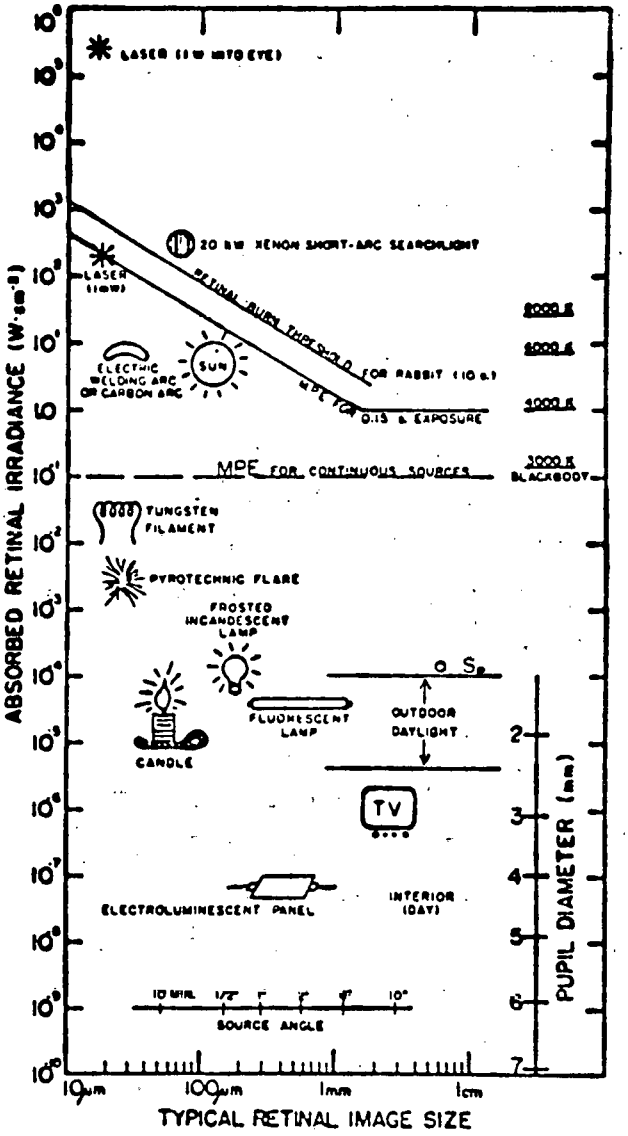

Figure 3. The eye is exposed to light sources having radiances varying from ~10^{4} W·cm^{-2}·sr^{-1} to ~10^{-6} W·cm^{-2}·sr^{-1} and less. The resulting retinal irradiances vary from ~200 W·cm^{-2} down to 10^{-7} W·cm^{-2} and even lower; retinal irradiances are shown for typical image sizes for several sources. A minimal pupil size was assumed for intense sources, except for searchlight. The retinal burn threshold for a 10-sec exposure of the rabbit retina[14] is shown as upper solid line. The maximum permissible exposure (MPE) applied by the U.S. Army Environmental Hygiene Agency in evaluating cw light sources is shown as lower solid line. Threshold for permanent shift of blue-cone sensitivity in monkeys obtained by Sperling is shown as O Sp at 3 x 10^{-4} W·cm^{-2}. Approximate pupil sizes are shown at lower right based upon exposure of most of the retina to light of the given irradiance. (Extracted from Sliney and Freasier[10])

The safe retinal irradiance for a 158-μ circular retinal image diameter (the same image that would result from viewing the sun) would be 12.66 W/cm^2 for momentary viewing. This safe E_r is about 150 percent of what would actually occur. Again, under most circumstances, there is a safety factor of 5 to 20 in these criteria.[10]

Clarence Robertson of Sandia Laboratories is perfecting a photographic method to directly assess retinal image size and irradiance simply by photographing the sun's image on the reflective surface and photographing the sun directly. But until more quantitative studies are performed that show these criteria to be too conservative, it would probably be advisable and reasonable to follow these accepted guidelines.

Multiple Beam Exposure Parameters

When dealing with many kinds of solar reflectors, there will be a finite possibility of multiple coincident beams (Diagram D). If the eye is exposed to this situation, the flux density is additive at the cornea as a function of the number of coincident beams. Due to the optical properties of the eye, the flux density on the retina is not increased. The total amount of energy that enters the eye and the total area of the retina that is exposed are increased, but the power density of solar radiation on the retina does not change since the images do not overlap.

If the eye is in coincident beams from widely separated sources, each retinal image will be separated and thermally independent of each other (Diagram E). There is some critical distance (which may also be a function of the specific power density of the images) between retinal images at which the separated incident energies can be dissipated by normal physiological mechanisms without having

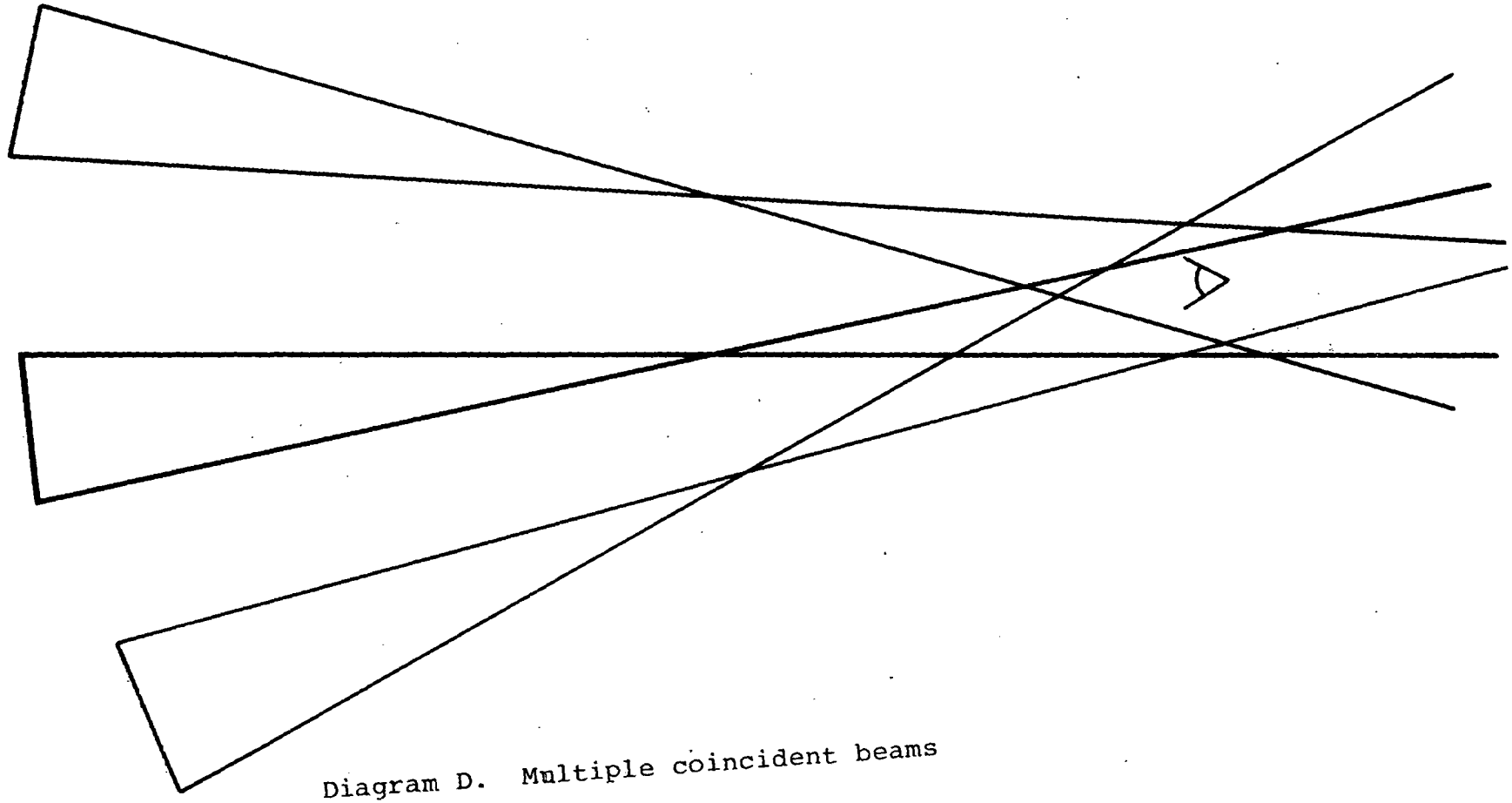

Diagram D. Multiple coincident beams

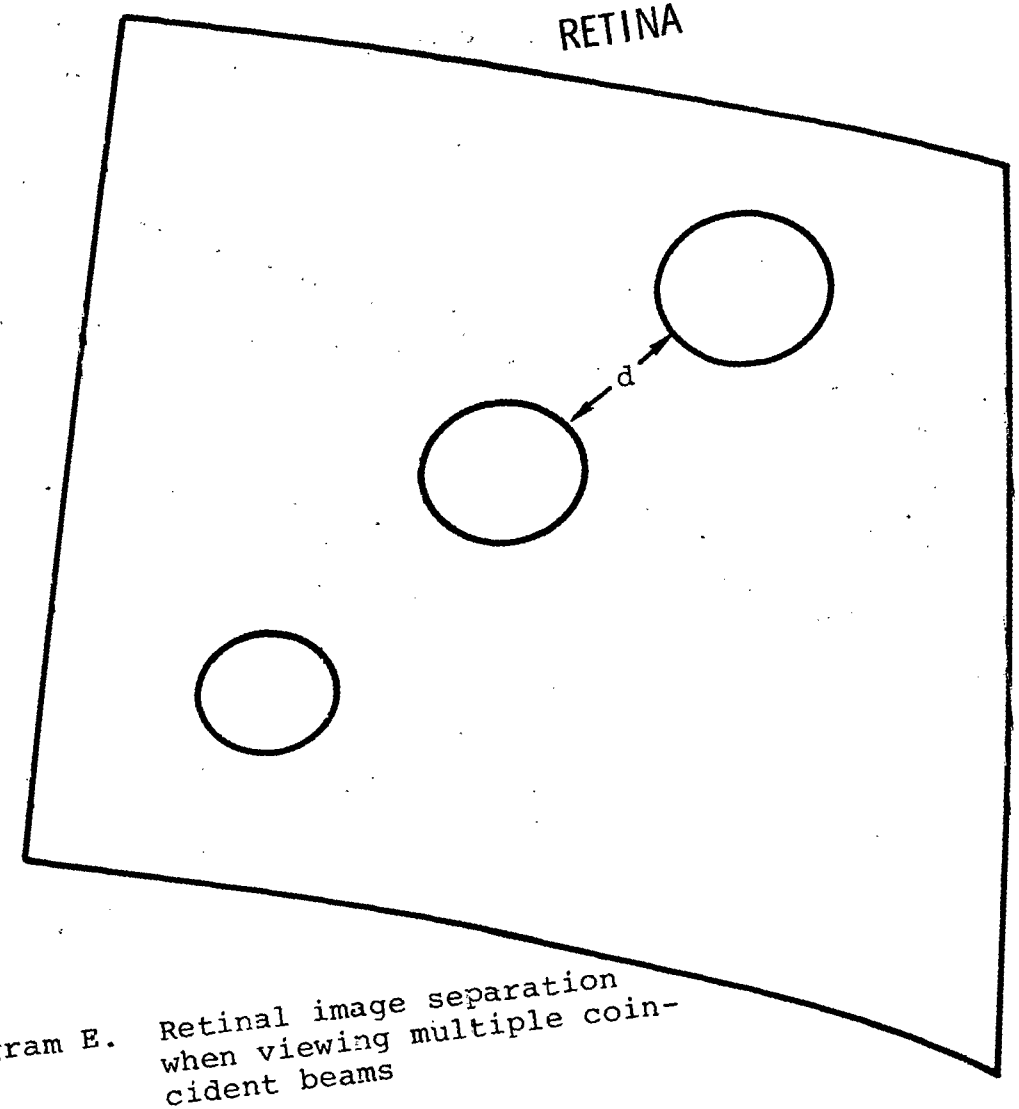

Diagram E. Retinal image separation when viewing multiple coincident beams

synergistic effects on each other. Equal to or greater than this critical distance the images are thermally independent. At less than this critical distance there is some mathematical relationship in the thermal properties of the images. The flux density is never additive because the images will never overlap.

To evaluate eye hazards from multiple solar reflecting sources, the following research needs to be performed:

1. Determine critical image separation distances on the retina as a function of image flux density for thermal and photochemical interaction between images.
2. Determine the mathematical relationships in the thermal and photochemical properties of retinal images separated by distances that are less than the critical distance as a function of flux density.
3. Determine chorioretinal burn threshold values for primates and maximum permissible exposure levels for multisource solar spectrum radiation with separated images greater than or equal to the critical distance separation (thresholds and MPEs should probably be the same as for single-source radiation), and separated images less than the critical distance separation.

Although we do not as yet have the needed information to measure eye hazards from multiple sources, an accepted procedure for eye-hazard analysis is to assume a worst-case condition. This very conservative scenario would group all images adjacent to each other to make a single large image that is the sum of all image areas.

From this assessment, decisions can be made using practical knowledge of the hazard, the equipment, and its intended use. T. D. Brumleve has used a similar approach to examine the eye hazard from heliostats at the 5-MW_t Solar Thermal Test Facility and to suggest beam-control criteria.[17]

Quantitative and empirical research is also needed on airplane pilot flashblindness from multisource solar spectrum radiation reflected from long focal length reflectors. Experiments will determine the retinal intensities a pilot can tolerate without impairing his flying ability. These criteria could also be used to evaluate hazards to motorists driving near the solar reflector.

Other Hazards to On-and Off-Site Personnel and Property

The hazard of erythema (sunburn) depends upon flux density and duration of exposure. Multiple sun corneal (skin) intensities would become sufficiently uncomfortable that evasive action would be quickly taken.[6] Fairly high flux levels could be tolerated for short reaction times (20 suns for 10 s)[18] as illustrated in Figure 4. The burn hazard from inadvertently touching the solar energy receiver or a hot fluid loop is greater than that resulting from a brief exposure to the reflected beam, except for exposure from within very close distances to the focal point.

To evaluate fire hazards from reflected solar flux, experiments by Sandia Laboratories [19,20,21] and others[22] suggest that easily combustible cellulosic materials such as dry brush and wood may be ignited by flux levels as low as 20 suns. Again, as evidenced in

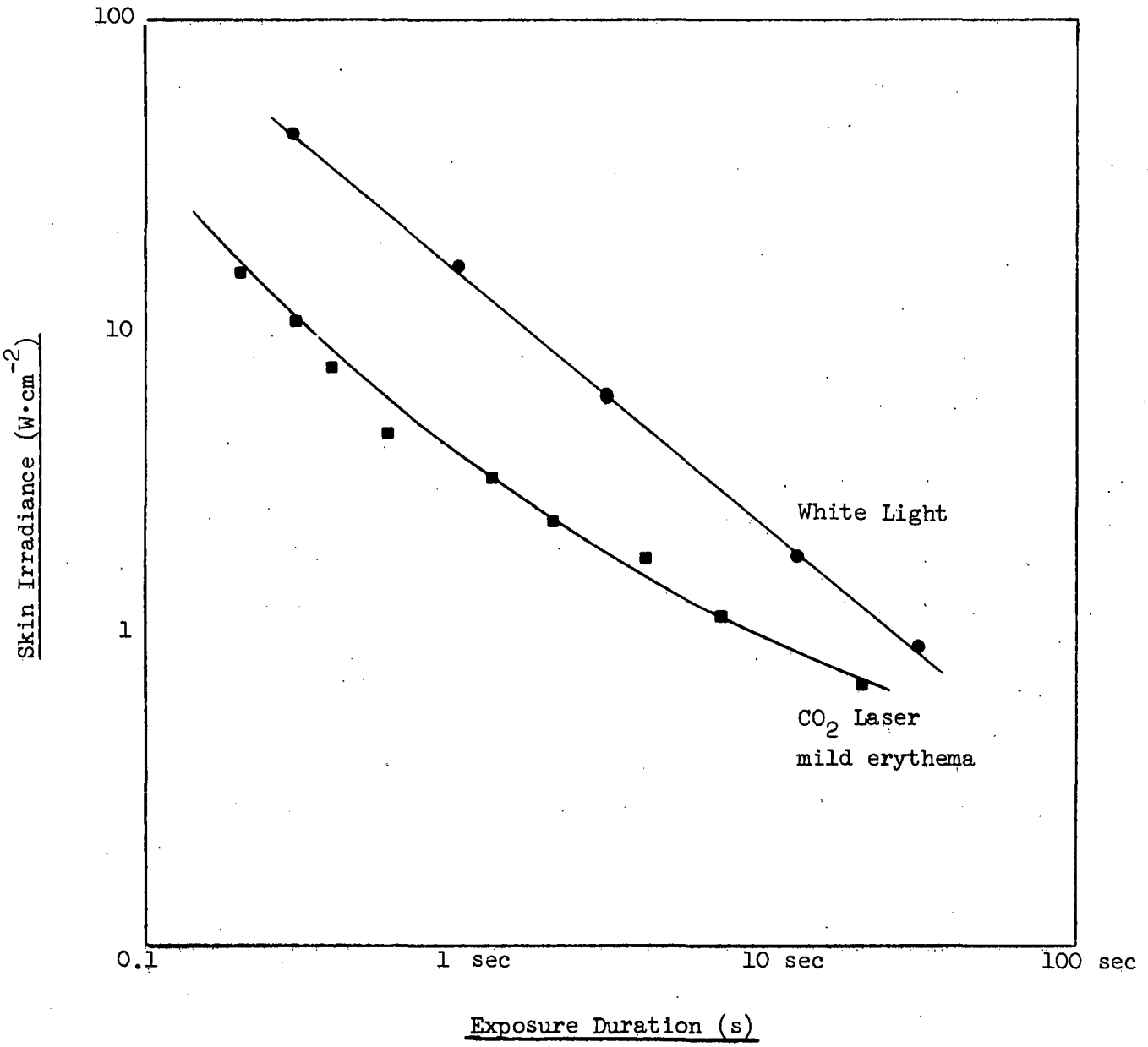

Figure 4. Pig skin injury data. Lower curve is for mildest erythema for 10.6 μm IR radiation. Upper curve is white-light first-degree burn threshold, as summarized by Davies.[18]

Reference 21, the hazard is time-dependent; that is, the higher the incident flux, the shorter the time that is necessary to cause ignition. But there does seem to be a level at which a fairly long exposure time is needed to initiate ignition.

Conclusion

Based on assumptions from Sliney and Freasier[10] we are reasonably able to predict the thermal chorioretinal maximum permissible exposure levels from a single-source solar spectrum radiation. These calculations provide information strongly suggesting that in many cases, exposures of personnel who are not near the focus and/or alignment point for blink-response exposures present a low hazard for biological damage, in most cases no worse than direct viewing of the sun.

Nonetheless, more work needs to be done. We need to refine the assumptions we are using. We need to perform basic and applied research to delineate more exact thresholds for the thermal as well as photochemical effects on single-and-multiple solar spectrum images. We need to concern ourselves with flashblindness as well as chorioretinal damage, and perhaps even lenticular, corneal, and iris damage for more chronic exposures.

Currently, action on these items is in progress or projected by Sandia Laboratories. In addition, mechanisms for protecting exposed personnel are being developed in software as well as hardware equipment.

We are far from being able to measure exactly all the unique safety and health hazards associated with solar energy collector and receiver systems. But we are making rapid progress. Research, especially in the area of eye hazards, is continuing; and more extensive work is planned.

References

1. Sandia Laboratories, SAND Vertical-Axis Wind Turbine Program, Albuquerque, New Mexico, 1977.

2. Sandia Laboratories, Solar Total Energy Test Facility, Albuquerque, New Mexico, 1977.

3. Sandia Laboratories, Solar Powered Irrigation, Albuquerque, New Mexico, 1977.

4. Sandia Laboratories, Photovoltaics at Sandia, Albuquerque, New Mexico, 1976.

5. Sandia Laboratories, Solar Thermal Test Facility, Albuquerque, New Mexico, 1977.

6. W. T. Ham, Jr. and D. H. Sliney, A Study of Optical Radiation Hazards Associated with a Solar Power Facility Proposal. Black and Veatch Consulting Engineers, August 16, 1976.

7. S. Duke-Elder and P. A. MacFaul, System of Ophthalamology, Vol. XIV, "Injuries, Part 2 Non-mechanical Injuries," 1972.

8. W. T. Ham, H. A. Mueller, R. C. Williams and W. J. Geeraets, "Ocular Hazard from Viewing the sun Unprotected and Through Various Windows and Filters," Appl. Opt. 12(9):2122-2129, September 1973.

9. W. T. Ham, H. Wiesinger, F. H. Schmidt, R. C. Williams, R. S. Ruffin and M. C. Sheffer, "Experimental Production of Flash Burns in the Rabbit Retina," Am. J. Ophth.,43:711-718, 1957.

10. D. H. Sliney and B. C. Freasier, "Evaluation of Optical Radiation Hazards," Applied Optic., Vol. 12, No. 1, January 1973.

11. J. C. Eccles and A. J. Flynn, "Experimental Photo-Retinitis," Med. J., Australia 1:339-342, 1944.

12. A. M. Clarke, Crit. Rev. Environ. Control, 1(3), 307, 1970.

13. W. T. Ham, W. J. Geeraets, R. C. Williams, D. Guerry and H. A. Mueller, in Proceedings of the First International Congress of Radiation Protection (Pergamon Prera, New York, 1968), pp 933 - 943.

14. A. M. Clarke, W. J. Geeraets and W. T. Ham, Appl. Opt., 8,1051, 1969.

References (Cont'd)

15. W. J. Geeraets, in Laser Eye Effects, H. G. Sperling Ed., Armed Forces - National Research Council Committee on Vision, AD697793 (Nat'l Tech. Information Service, Springfield, VA 22151), 1968.

16. T. J. White, M. A. Mainster, P. W. Wilson and J. H. Tips, "Chorioretinal Temperature Increases from Solar Observation," Bulletin of Mathematical Biophysics, 33:1-17, 1971.

17. T. D. Brumleve, Eye Hazard and Glint Evaluation for the 5-MW Thermal Test Facility, Sandia Laboratories, Albuquerque, New Mexico, May 1977.

18. J. M. Davies, The Effect of Intense Thermal Radiation on Animal Skin, A Comparison of Calculated and Observed Burns, Report T-24, Army Quartermaster Research and Engineering Command, Nateck, MA AD456794, April 29, 1959.

19. L. L. Young, to Distribution, Sixteen-inch Telescopic Mirror Brush Fire Experiment, Sandia Laboratories, Albuquerque, New Mexico, March 2, 1977.

20. L. K. Matthews and L. L. Young to J. V. Otts, Intensity Necessary for Combustion of Wood, Sandia Laboratories, Albuquerque, New Mexico, May 3, 1977.

21. L. K. Matthews and L. L. Young to J. V. Otts, Fire Hazard of Tower Test Bay Wood During VIP Demo, Sandia Laboratories, Albuquerque, New Mexico, May 5, 1977.

22. D. L. Simms, "Ignition of Cellulosic Materials by Radiation," Combustion and Flame 4:294-300, 1960.

DISTRIBUTION:

US Department of Energy
Division of Headquarters Services
Library Branch Room G-049
Washington, DC 20545

US Department of Energy
Albuquerque Operations Office
P. O. Box 5400
Albuquerque, NM 87115
Attn: J. R. Roeder

US Department of Energy
San Francisco Operations Office
1333 Broadway
Wells Fargo Building
Oakland, CA 94612
Attn: J. T. Davis

Los Alamos Scientific Laboratory
Safety Group H-3
Mail Stop 403
Los Alamos, NM 87545
Attn: Jack Bacaston

Texas Instruments Incorporated
Radiation Safety
P. O. Box 5474
Mail Stop 262
Dallas, Tx 75222
Attn: R. H. Kinslow

Bell Telephone Laboratories
Safety Office
Holmdel, NJ
Attn: J. C. Berka

John & Higgins
95 Wall Street
New York, NY 10005

Schering-Plough Corp
60 Orange Street
Bloomfield, NJ 0700
Attn: J. M. Galat

John N. Romine & Associates
1631 Sheridan Road
Bartlesville, OK 74003

Brookhaven National Laboratory
Building 535
Upton, NY 11973
Attn: Herb Schulman

3311 D. R. Parker
Attn: W. Stocum
3161 R. P. Gall (2)
3440 L. M. Jercinovic
3442 D. L. Rost
5000 A. Narath
5231 C. M. Vittitoe
5231 F. Biggs
5700 J. H. Scott
5710 G. E. Brandvold (10)
8132 T. D. Brumleve
8252 P. K. Lovell
Attn: H. Lucas
9412 C. E. Robertson
3442 L. L. Young (40)
3141 C. A. Pepmuller (Actg) (5)
3151 W. L. Garner (3)
For: DOE/TIC
(Unlimited Release)

DOE/TIC (25)
(R. P. Campbell, 3172-3)